



# In-situ synthesis and ultrasound enhanced adsorption properties of MoS<sub>2</sub>/graphene quantum dot nanocomposite

Congxu Wang<sup>a,b</sup>, Jianli Jin<sup>a,b</sup>, Youyi Sun<sup>a,b,\*</sup>, Junru Yao<sup>a,b</sup>, Guizhe Zhao<sup>a</sup>, Yaqing Liu<sup>a,b,\*</sup>

<sup>a</sup> Shanxi Province Key Laboratory of Functional Nanocomposites, North University of China, Taiyuan 030051, PR China

<sup>b</sup> School of Materials Science and Technology, North University of China, Taiyuan 030051, PR China

## HIGHLIGHTS

- The MoS<sub>2</sub>/GOD was successfully synthesized through a one-step hydrothermal approach.
- The MoS<sub>2</sub>/GOD as adsorbents showed ultrafast adsorption rate under ultrasound.
- The adsorption properties of MoS<sub>2</sub>/GOD were not depended on temperature and pH.

## ARTICLE INFO

### Article history:

Received 28 April 2017

Received in revised form 27 June 2017

Accepted 27 June 2017

Available online 28 June 2017

### Keywords:

MoS<sub>2</sub>/GQD

In-situ synthesis

Absorbent

Ultrasound

Ultrafast adsorption rate

## ABSTRACT

The MoS<sub>2</sub>/graphene quantum dot nanocomposite (MoS<sub>2</sub>/GQD) was successfully synthesized through a one-step hydrothermal approach and then directly applied as the adsorbents for removing organic dyes from water. It showed excellent adsorption capacity (285.0 mg/g) and ultrafast adsorption rate (2 s) under ultrasound assistance. Furthermore, the MoS<sub>2</sub>/GQD exhibited high cycling stability and the adsorption capacity of MoS<sub>2</sub>/GQD was slightly affected by the temperature and pH of solution. These results were attributed to the high porous structure and large surface area of the MoS<sub>2</sub>/GQD, which provided more volume and surface area for the adsorption organic dyes and enabled highly accessible to the organic dyes under ultrasound assistance. This work did not only indicate the great potential of MoS<sub>2</sub>/GQD as adsorbents in water pollution treatment, but also provided a new idea for improving the adsorption rate of adsorbents in water pollution treatment.

© 2017 Elsevier B.V. All rights reserved.

## 1. Introduction

In past several decades, organic dyes in water was more and more serious due to that textile industries, chemical plant and other related enterprise often let pollutant into rivers [1]. These organic pollutants did not only consume dissolved oxygen and menace aquatic in water, but also endanger human health [2]. Therefore, it was very important for developing a low cost and high efficient method to remove the organic dyes from water, such as adsorption, photo-degrading chemical oxidation and electrochemical processes [3–7]. Among mentioned above, the adsorption technique was most effective and economical ways to remove organic dyes from water [8]. It was well-known that the properties of adsorbents was the key role for the adsorption technique. In previous works, various materials, such as clay, zeolites, SiO<sub>2</sub>, Al<sub>2</sub>O<sub>3</sub>, carbon materials, MoS<sub>2</sub> and ion exchange resins have widely acted as

adsorbents for application in adsorption technique [8–19]. Despite there were lots of works reported the synthesis and properties of adsorbents applied in removing organic dyes from water, however, it was still a large challenge for these adsorbents with high adsorption capacity and high adsorption rate, together. Especially, the low adsorption rate of adsorbents with high adsorption capacity restricted its practical application. In addition to this, the adsorption capacity of adsorbents generally depended on the temperature and pH of solution, leading to additional cost and time. So, it was also interesting to find a new adsorbent, in which the adsorption capacity was slightly affected by the temperature and pH. Layered MoS<sub>2</sub> structures possessed significant adsorption ability, which was useful for further research and practical applications of the layered MoS<sub>2</sub> adsorbent in wastewater treatment [15,20–25].

Herein, the a new adsorbent based on MoS<sub>2</sub> and GQD was designed and synthesized by a facile method. Furthermore, the effect of ultrasound on adsorption properties of the adsorbent was investigated in detail. Owing to the unique porous morphology and ultrasound assistant, the new adsorbent showed signifi-

\* Corresponding authors at: Shanxi Province Key Laboratory of Functional Nanocomposites, North University of China, Taiyuan 030051, PR China.

E-mail addresses: [syyi@pku.edu.cn](mailto:syyi@pku.edu.cn) (Y. Sun), [lyqgz2010@163.com](mailto:lyqgz2010@163.com) (Y. Liu).

cant high adsorption capacity, ultrafast adsorption rate and high cycle adsorption stability. These did not only prove to synthesize a new adsorbent with high performance, but also provide a new method for improving the adsorption rate of adsorbent.

## 2. Experiment

### 2.1. Reagents and solutions

All the chemical reagents used in this work were of analytic grade and commercially available unless otherwise noted. The deionized water (obtained from a Milli-Qplus 185 equip) was used through the experiments. All salts (hexaammonium heptamolybdate tetrahydrate, thiourea, glucose, Rhodamine B (RhB), methylene blue (MB) and methyl orange (MO)) were purchased from Aladdin Industrial Corporation.

### 2.2. Synthesis of the adsorbent based on MoS<sub>2</sub> and GQD

The adsorbent was synthesized by one-step hydrothermal method as shown in following. 1.24 g hexaammonium heptamolybdate tetrahydrate, 2.28 g thiourea and 1.0 g glucose were dissolved in 40 ml deionized water to form homogeneous solution by vigorous stirring. Then the mixture was transferred into a Teflon-lined stainless steel autoclave, which was further heated at 220 °C for 12 h. After the autoclave cooled down to room temperature, the black precipitates were collected by centrifugation (12,000 rpm, 5 min) and washed with distilled water and ethanol for three times, respectively. For a comparison, the MoS<sub>2</sub> was also synthesized at the same process.

### 2.3. Characterizations

The crystalline structure of products was determined by the X-ray diffraction (HAOYUAN, 2700B) using Cu K $\alpha$  ( $\lambda = 0.1546$  nm). The morphology and size of products was characterized by the Scanning electron microscopy (SEM, Su-8100) with energy-dispersive spectra and energy-dispersive X-ray spectrometer. The morphology of products was also characterized by Transmission electron microscopy (TEM, JEM-2100f) at an acceleration voltage of 200 kV. The chemical structure of products was characterized by the Fourier transform infrared spectrophotometer (Thermo Nicolet 360).

### 2.4. Adsorption treatment

The adsorption properties of adsorbent based on MoS<sub>2</sub> and GQD was determined by removing dyes (RhB, MO and MB) from water. The adsorption process was shown in following. 20.0 mg adsorbent was added to 50.0 ml dye solution (30.0 mg/L–200.0 mg/L) under stirring and ultrasound. At the same time, the 3.0 ml mixing solution was took out at various treatment time. Here, treatment time was obtained with a *stop-watch*. The adsorbents was removed from 3.0 ml mixing solution by the *centrifugating* method. And then, the supernate was analyzed by UV–vis spectra. The recyclability of the adsorbent was also investigated with the same process. The adsorption capacity  $q_t$  (mg/g) and removal rate (Removal%) was calculated according to the following formulas.

$$q_t = \frac{(C_0 - C_t)V}{m} \quad (1)$$

$$\text{Removal} = \frac{C_0 - C_t}{C_0} \times 100\% \quad (2)$$

where  $C_0$  and  $C_t$  were the dye initial concentration (mg/L) and dye concentration (mg/L) treated with time  $t$ , respectively. The  $V$  and  $m$

was the volume (L) of dye solution and mass (mg) of adsorbent, respectively.

## 3. Results and discussion

The formation of MoS<sub>2</sub> and MoS<sub>2</sub>/GQD was firstly confirmed by the XRD as shown in Fig. 1. From the XRD pattern of pure MoS<sub>2</sub>, three broad diffuse-like peaks at 16°, 33° and 58° were assigned to the (002), (100) and (110) planes of MoS<sub>2</sub>, respectively, which was in good agree with the reported data for MoS<sub>2</sub> and were well indexed to the standard cubic phase of MoS<sub>2</sub> (JCPDS Card no. 37-1492) [20]. For a comparison, the similar (002), (100) and (110) planes of MoS<sub>2</sub> were also presented in XRD pattern of the MoS<sub>2</sub>/GQD [26], indicating that the crystal phase of MoS<sub>2</sub> was not change after introduction of GQD. At the same time, the characteristic peaks of GQD were not observed due to be low doping content and low crystallite, which was similar with previous work [26]. In addition to this, no peaks corresponding to impurities were detected. These results confirmed the formation of MoS<sub>2</sub> and MoS<sub>2</sub>/GQD with high purity.

The morphology of MoS<sub>2</sub> and MoS<sub>2</sub>/GQD was determined by the FE-SEM images as shown in Fig. 2. As shown in Fig. 2A, the MoS<sub>2</sub>/GQD showed the fungus-like nanosheet structure, demonstrating that the obtained product consisted of large-scale uniform nanosheets. It also clearly showed that the thickness of MoS<sub>2</sub> nanosheets was about 15.0 nm. In a comparison, the pure MoS<sub>2</sub> showed spherical shapes composed of nanosheets and its diameter was about 1.0  $\mu\text{m}$  as shown in Fig. 2B. The results indicated that the morphology of MoS<sub>2</sub> was change after introduction of GQD. The elemental mapping images of MoS<sub>2</sub>/GQD and MoS<sub>2</sub> were characterized and compared as shown in Fig. 2C and D, respectively. As seen from Fig. 2C, it clearly revealed Mo, S and C elements to be uniform distribution in the MoS<sub>2</sub>/GQD. Contrarily, it also showed Mo and S elements, but the C elements were not observed for MoS<sub>2</sub> as shown in Fig. 2D. Energy-dispersive X-ray spectrometer (EDS) of MoS<sub>2</sub>/GQD and pure MoS<sub>2</sub> were also characterized as shown in Fig. 2E and F, respectively. It clearly presented Mo and S elements for all samples, in which the calculated atomic ratio of Mo to S was close to 1:2. In addition to this, excluding the peaks assigned Mo and S element, a new peak centered at 0.12 keV appeared for MoS<sub>2</sub>/GQD, corresponding to the C element of GQD. According to the weight ratio of C, Mo and S element, the content of GQD was calculated to be about 5.6 wt% for MoS<sub>2</sub>/GQD. At the same time, no peaks corresponding to other elements were

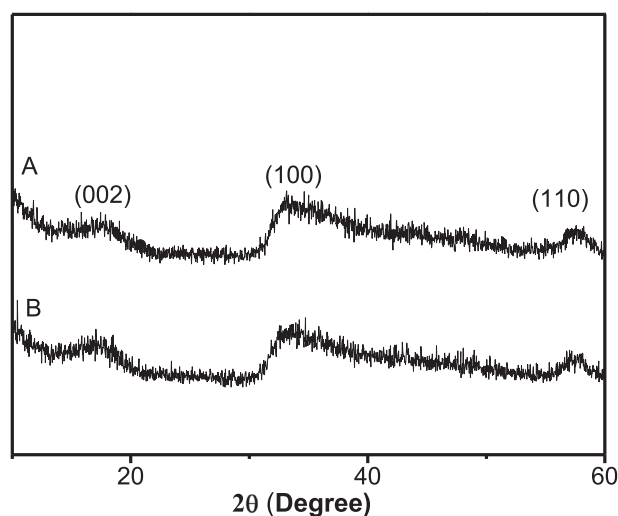


Fig. 1. XRD patterns of (A) MoS<sub>2</sub> and (B) MoS<sub>2</sub>/GQD.

Download English Version:

<https://daneshyari.com/en/article/6465085>

Download Persian Version:

<https://daneshyari.com/article/6465085>

[Daneshyari.com](https://daneshyari.com)